Cancer Cell
Article

Targeted Activation of Human Vγ9Vδ2-T Cells Controls Epstein-Barr Virus-Induced B Cell Lymphoproliferative Disease

Zheng Xiang,[1,9] Yinping Liu,[1,9] Jian Zheng,[1] Ming Liu,[2] Aizhen Lv,[1] Yulong Gao,[1] Huaidong Hu,[3] Kowk-Tai Lam,[1] Godfrey Chi-Fung Chan,[1] Yuanzhong Yang,[4] Honglin Chen,[5] George Sai-Wah Tsao,[6] Marc Bonneville,[7,8,10] Yu-Lung Lau,[1] and Wenwei Tu[1,*]

[1]Department of Paediatrics and Adolescent Medicine, Li Ka Shing Faculty of Medicine, University of Hong Kong, Hong Kong, China
[2]Guangzhou Institute of Respiratory Diseases, Guangzhou Medical College, Guangzhou, China
[3]Key Laboratory of Molecular Biology for Infectious Diseases, Ministry of Education, The Second Affiliated Hospital of Chongqing Medical University, Chongqing, China
[4]Department of Pathology, Sun Yat-Sen University Cancer Center, Guangzhou, China
[5]Department of Microbiology, Li Ka Shing Faculty of Medicine, University of Hong Kong, Hong Kong, China
[6]Department of Anatomy, Li Ka Shing Faculty of Medicine, University of Hong Kong, Hong Kong, China
[7]Centre de Recherche en Cancérologie Nantes-Angers, Université de Nantes, 44300 Nantes, France
[8]INSERM U892 CNRS UMR6299, 44300 Nantes, France
[9]Co-first author
[10]Present address: Institut Mérieux, 17 rue Bourgelat 69002 Lyon, France
*Correspondence: wwtu@hku.hk
http://dx.doi.org/10.1016/j.ccr.2014.07.026

SUMMARY

Epstein-Barr virus-induced lymphoproliferative disease (EBV-LPD) after transplantation remains a serious and life-threatening complication. Herein we showed that the aminobisphosphonate pamidronate-expanded human Vγ9Vδ2-T cells efficiently killed EBV-transformed autologous lymphoblastoid B cell lines (EBV-LCL) through γ/δ-TCR and NKG2D receptor triggering and Fas and TRAIL engagement. By inoculation of EBV-LCL in Rag2$^{-/-}$γc$^{-/-}$ mice and humanized mice, we established lethal EBV-LPD with characteristics close to those of the human disease. Adoptive transfer of pamidronate-expanded Vγ9Vδ2-T cells alone effectively prevented EBV-LPD in Rag2$^{-/-}$γc$^{-/-}$ mice and induced EBV-LPD regression in EBV^{+} tumor-bearing Rag2$^{-/-}$γc$^{-/-}$ mice. Pamidronate treatment inhibited EBV-LPD development in humanized mice through selective activation and expansion of Vγ9Vδ2-T cells. This study provides proof-of-principle for a therapeutic approach using pamidronate to control EBV-LPD through Vγ9Vδ2-T cell targeting.

INTRODUCTION

Epstein-Barr virus (EBV) is a herpesvirus that latently infects human B cells in most individuals by adulthood. Persistent EBV infection is generally subclinical in immunocompetent hosts (Cohen, 2000). However, immunocompromised patients are at high risk of developing EBV-induced B cell lymphoproliferative disorders (EBV-LPD) with significant morbidity and mortality (Shapiro et al., 1988). Current treatment options for EBV-LPD include restoring the cellular immune responses to EBV and depleting the B cells with monoclonal antibodies or chemotherapy (Heslop et al., 2010; Khanna et al., 2005; Wagner-Johnston and Ambinder, 2007). Restoration of cellular immune responses by adoptive transfer of ex vivo-generated EBV-specific cytotoxic T lymphocytes (CTL) has yielded promising results for treatment of EBV-LPD (Kanakry and Ambinder,

Significance

Current treatment strategies for EBV-LPD include restoring EBV-specific cytotoxic T lymphocytes (CTL) and depleting the B cells with monoclonal antibodies or chemotherapy. However, restoration of EBV-specific CTL is limited by the difficulties in generating enough numbers of EBV-specific CTL in vitro and the lack of in vivo expansion of infused CTL. Antibody-mediated targeting EBV-infected B cells and chemotherapy have unwanted side effects and lead to general immunosuppression. We reveal herein that the aminobisphosphonate pamidronate can control EBV-LPD by enhancing human Vγ9Vδ2-T cell immunity. Because pamidronate has been already used for decades in osteoporosis treatment, this "new application of an old drug" potentially offers a safe and readily available option for the treatment of EBV-LPD.

2013; Khanna et al., 1999; Leen et al., 2007; Long et al., 2011; Rooney et al., 1995). However, its application for the treatment of EBV-LPD is limited by the difficulties in generating enough numbers of EBV-specific CTL in vitro and the lack of in vivo expansion of infused CTL in patients with bulky disease (Leen et al., 2007; Louis et al., 2009). Antibody-mediated targeting EBV-infected B cells has unwanted side effects because anti-CD20 antibody also depletes normal B cells causing prolonged hypogammaglobulinemia, and chemotherapy has unwanted off-target toxicity and also causes general immunosuppression (Leen et al., 2007). Thus, there is an urgent need for developing better strategies to control EBV-LPD.

γδ-T cells are considered as the innate-like T lymphocytes with natural killer (NK) cell characteristics (Born et al., 2006; Carding and Egan, 2002). Various innate signals, either alone or in combination with ligand recognition via the T-cell receptor, induce γδ-T cells to display innate-like immune functions (Bonneville and Scotet, 2006; Born et al., 2006; Zheng et al., 2013a). γδ-T cells make up 1%–10% of T lymphocytes in the blood and peripheral organs in adult humans. Most γδ-T cells in the peripheral blood and lymphoid organs of healthy human adults are Vγ9Vδ2-T cells. Vγ9Vδ2-T cells can be specifically activated in an HLA-unrestricted manner by small nonpeptidic phosphoantigens, which are metabolites of isoprenoid biosynthesis pathways (Beetz et al., 2008). Isopentenyl pyrophosphate (IPP), an intermediate produced through the mevalonate pathway, was found to selectively activate and expand human Vγ9Vδ2-T cells in vitro and in vivo (Alexander et al., 2008; Puan et al., 2007). Pharmacological compounds, such as the aminobisphosphonate pamidronate commonly used for the treatment of osteoporosis, can induce intracellular accumulation of IPP, leading to activation and expansion of human Vγ9Vδ2-T cells (Bonneville and Scotet, 2006). Human Vγ9Vδ2-T cells can exert broad antiviral and antitumor activities in vitro and in humanized mice in vivo (Fournié et al., 2013; Qin et al., 2011, 2012; Tu et al., 2011). However, whether these cells have similar effects on EBV and EBV-LPD remains unknown.

Recently we established humanized mice with human peripheral blood mononuclear cells (huPBMC). These mice contain functional human T and B cells, including a similar percentage of Vγ9Vδ2-T cells in peripheral blood as seen in human (Tu et al., 2011; Zheng et al., 2013b). In this study, we investigated the effect of pamidronate-expanded human Vγ9Vδ2-T cells on the growth of EBV-transformed autologous lymphoblastoid B cell lines (EBV-LCL) in vitro and in immunodeficient $Rag2^{-/-}\gamma c^{-/-}$ mice, and further determined the role of pamidronate in the control of EBV-LPD in humanized mice.

RESULTS

Vγ9Vδ2-T Cells Kill EBV-LCL In Vitro

EBV-LCL showed enhanced expression of stress-inducible major histocompatibility complex class I-related proteins A and B (MICA/B), Fas, and tumor necrosis factor-related apoptosis-inducing ligand (TRAIL) receptor 2 (DR5) expression when compared to their normal autogolous B cells (Figure 1A). In contrast, both normal B cells and EBV-LCL had little or no Fas ligand (FasL) and TRAIL receptor 1 (DR4) expression on the cell surface (Figure 1A). Consistent with our previous reports (Li et al., 2013; Tu et al., 2011), pamidronate induced selective activation and expansion of Vγ9Vδ2-T cells, and upregulation of the surface expressions of CD69, NKG2D, FasL, TRAIL, and intracellular cytolytic granules, perforin and granzyme B, in Vγ9Vδ2-T cells (Figures S1A–S1D available online). In contrast, EBV-LCL alone could not efficiently expand Vγ9Vδ2-T cells from EBV-seropositive donors (Figures S1E and S1F).

Pamidronate-expanded Vγ9Vδ2-T cells were purified by positive or negative selection with anti-TCRγ/δ MicroBead or TCRγ/δ^+ T cell isolation kit, and then co-cultured with autologous EBV-LCL. As shown in Figure 1B, pamidronate-expanded Vγ9Vδ2-T cells sorted through negative selection only had minor cytotoxic activity against EBV-LCL, whereas pamidronate-expanded Vγ9Vδ2-T cells sorted through positive selection had significant higher cytotoxic activity against EBV-LCL. In addition, Vγ9Vδ2-T cells sorted through positive selection had higher CD69, Fas, FasL, TRAIL, and granzyme B expressions than those sorted through negative selection (Figure S1G). These results indicated that recent γ/δ-T cell receptor (TCR) engagement enhanced their activation and cytotoxicity against EBV-LCL.

Pamidronate-expanded Vγ9Vδ2-T cells sorted through positive selection displayed potent cytotoxicity against EBV-LCL in a dose-dependent manner, but showed limited if any killing activity against normal B cells (Figure 1C). This cytotoxicity required cell-cell direct contact, as indicated by Transwell experiments (Figure 1D). The immobilized recombinant MICA/B enhanced Vγ9Vδ2-T cell activation, especially for the cells sorted through positive selection, in terms of the expressions of CD69, NKG2D, Fas, FasL, TRAIL, perforin, or granzyme B (Figure S1G). The significant granule exocytosis, as evidenced by the increase of surface expression of CD107a, was also detected in Vγ9Vδ2-T cells upon the immobilized MICA/B stimulation (Figure 1E). In parallel with granule exocytosis, the immobilized MICA/B significantly enhanced the cytotoxic activity of Vγ9Vδ2-T cells against EBV-LCL (Figure 1F). Indeed, the levels of the granule exocytosis and cytotoxicity of Vγ9Vδ2-T cells sorted through positive selection were much higher than that in cells sorted through negative selection upon the immobilized MICA/B stimulation (Figures 1E and 1F). These data suggest MICA/B expressed EBV-LCL can enhance the activation and cytotoxic activity of Vγ9Vδ2-T cells especially those sorted through positive selection. Therefore, pamidronate-expanded Vγ9Vδ2-T cells purified with γ/δ-TCR positive selection were used for subsequent experiments.

Blockade of NKG2D, FasL, and TRAIL using appropriate neutralizing antibodies significantly inhibited the cytolytic activities of Vγ9Vδ2-T cells against EBV-LCL (Figure 1G). To confirm the involvement of cytolytic granule release in the killing of EBV-LCL by Vγ9Vδ2-T cells, the perforin-specific inhibitor concanamycin A (CMA) and granzyme B inactivator Bcl-2 were used. As shown in Figure 1G, cytolytic activity of Vγ9Vδ2-T cells against EBV-LCL was strongly inhibited after CMA or Bcl-2 treatment. These results indicate that the cytotoxicity of Vγ9Vδ2-T cells against EBV-LCL depends on NKG2D activation, and is mediated by Fas-FasL, TRAIL-DR5, and perforin-granzyme B pathways. In addition, pamidronate alone did not show any cytotoxic activities against EBV-LCL (Figures S1H and S1I), but it could enhance the expression of EBV-LCL recognition receptors and cytotoxic molecules in Vγ9Vδ2-T cells (Figure S1J). Taken

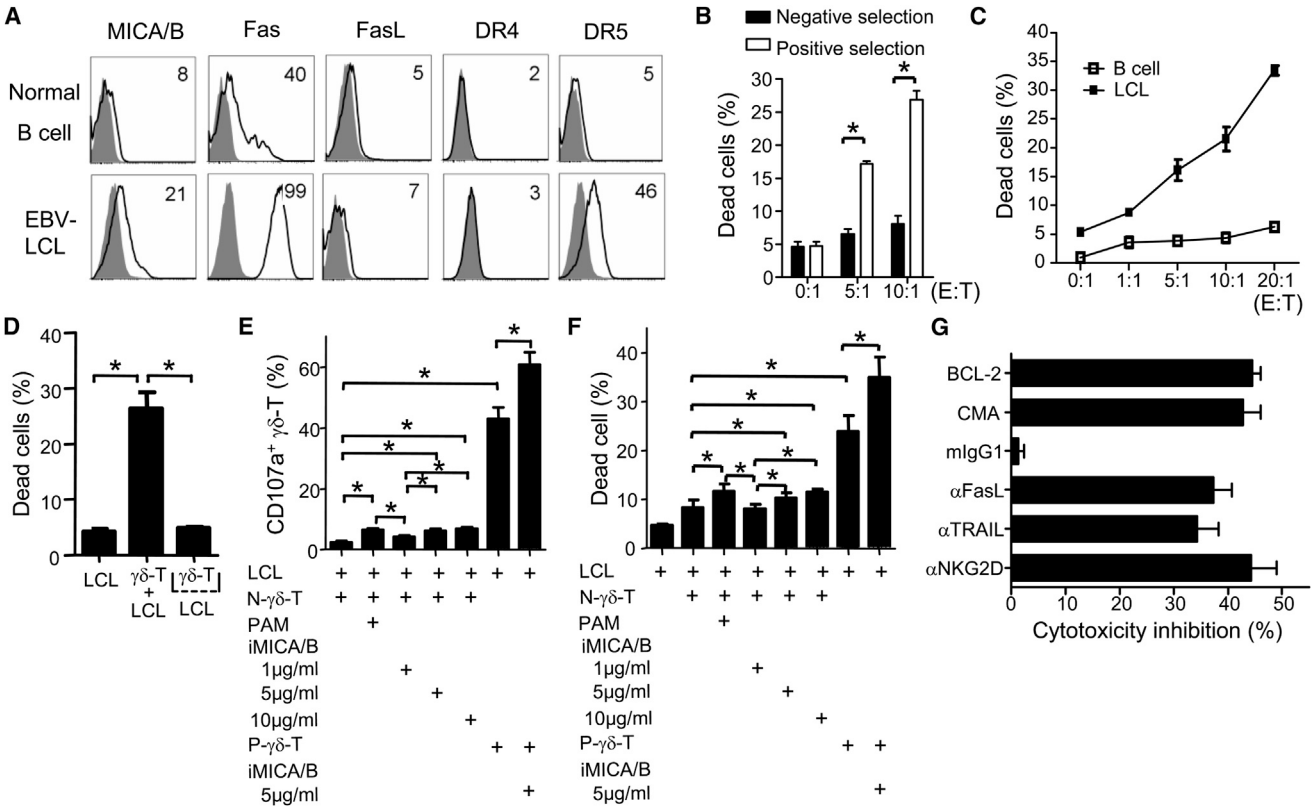

Figure 1. Vγ9Vδ2-T Cells Kill EBV-LCL In Vitro

(A) Phenotypes of EBV-LCL and autologous normal human B cells. The white histograms represent MICA/B, Fas, FasL DR4 and DR5, and the gray histograms represent isotype controls. (B, E, and F) Pamidronate (PAM)-expanded Vγ9Vδ2T cells were purified by positive selection (P-γδ-T) or negative selection (N-γδ-T) with anti-TCRγ/δ MicroBead or TCRγ/δ$^+$ T cell isolation kit, and then cultured with the autologous EBV-LCLs at different ratios for 4 hr. (C, D, and G) PAM-expanded Vγ9Vδ2T cells purified by positive selection were cocultured with autologous EBV-LCL or normal B cells at different E:T ratios (C) or an E:T ratio of 10:1 (D and G) for 4–6 hr. (D) The Vγ9Vδ2T cells were directly cocultured with or physically separated from autologous EBV-LCLs for 6 hr by using a transwell system. (E and F) P-γδ-T or N-γδ-T cells were pretreated with or without immobilized MICA/B for 6 hr, and then cocultured with autologous EBV-LCL at an E:T ratio of 10:1 for 4–6 hr. The percentages of dead cells among whole target cells (CD3$^-$ population) identified as CD3$^-$ PI$^+$ (B–D and F) and the surface expression of CD107a on Vγ9Vδ2T cells (E) are shown. (G) The perforin inhibitor CMA, granzyme B inactivator Bcl-2, anti-NKG2D (αNKG2D), anti-TRAIL (αTRAIL), and anti-FasL (αFasL) blocking antibodies, or their relevant isotype control (mouse IgG1, mIgG1) were used in coculture of EBV-LCL and their autologous PAM-expanded Vγ9Vδ2T cells. The cytotoxicity was shown as the percentage of inhibition relative to those without any treatment. All the data shown as mean ± SEM are representative of four independent experiments. *$p < 0.05$. See also Figure S1.

together, our results indicated that pamidronate-expanded Vγ9Vδ2-T cells can efficiently kill EBV-LCL.

Vγ9Vδ2-T Cells Prevent EBV-LPD in Rag2$^{-/-}$γc$^{-/-}$ Mice

Human B cells infected with the EGFP-tagged EBV were used to establish EGFP$^+$ EBV-LCL to monitor the growth of EBV-LCLs in vivo. The EBV-LPD model was further established in the Rag2$^{-/-}$γc$^{-/-}$ immunodeficient mice after subcutaneous (s.c.) inoculation of EGFP-expressing EBV-LCL (0.1×10^6/mouse; Figure 2A; Lacerda et al., 1996). To determine whether human Vγ9Vδ2-T cells could prevent EBV-LPD in vivo, highly purified (>97%) pamidronate-expanded autologous Vγ9Vδ2-T cells (10×10^6 cells/mouse) were adoptively transferred intravenously (i.v.) into Rag2$^{-/-}$γc$^{-/-}$ mice at days 0, 7, 14, and 21 after EGFP-expressing EBV-LCL inoculation (Figure 2A). PBS-treated mice were used as controls.

After inoculation with EBV-LCL, EBV-LPD developed in all control mice. The rapid growth of EBV-LCL was detected subcutaneously in PBS-treated mice by in vivo imaging after inoculation with EBV-LCL (Figure 2B), and subcutaneous solid tumors developed in all control mice (Figures 2B and C). Histologically, these tumors were immunoblastic lymphomas and derived from human B cells as evidenced by positive staining for human CD20 (Figure 2D). The tumor cells had high expression levels of EBV latent membrane protein 1 (LMP1) and small EBV-encoded RNAs type 1/2 (EBER-1/2) expressions (Figure 2D). Furthermore, tumor metastases in liver, kidney, and lung were evidenced by histological and immunophenotypic analysis for CD20, LPM1, and EBER-1/2 expression (Figure 2E). As a result, 9 of 11 (82%) PBS-treated mice died within 60 days after EBV-LCL inoculation (Figure 2F).

Adoptive transfer of Vγ9Vδ2-T cells significantly enhanced survival of EBV-LCL-grafted immunodeficient mice (Figure 2F). Indeed only 1 of 10 mice with adoptively transferred Vγ9Vδ2-T cells died during the 100 day-observation period (Figure 2F), and subcutaneous solid tumors developed in only 2 of 10 mice

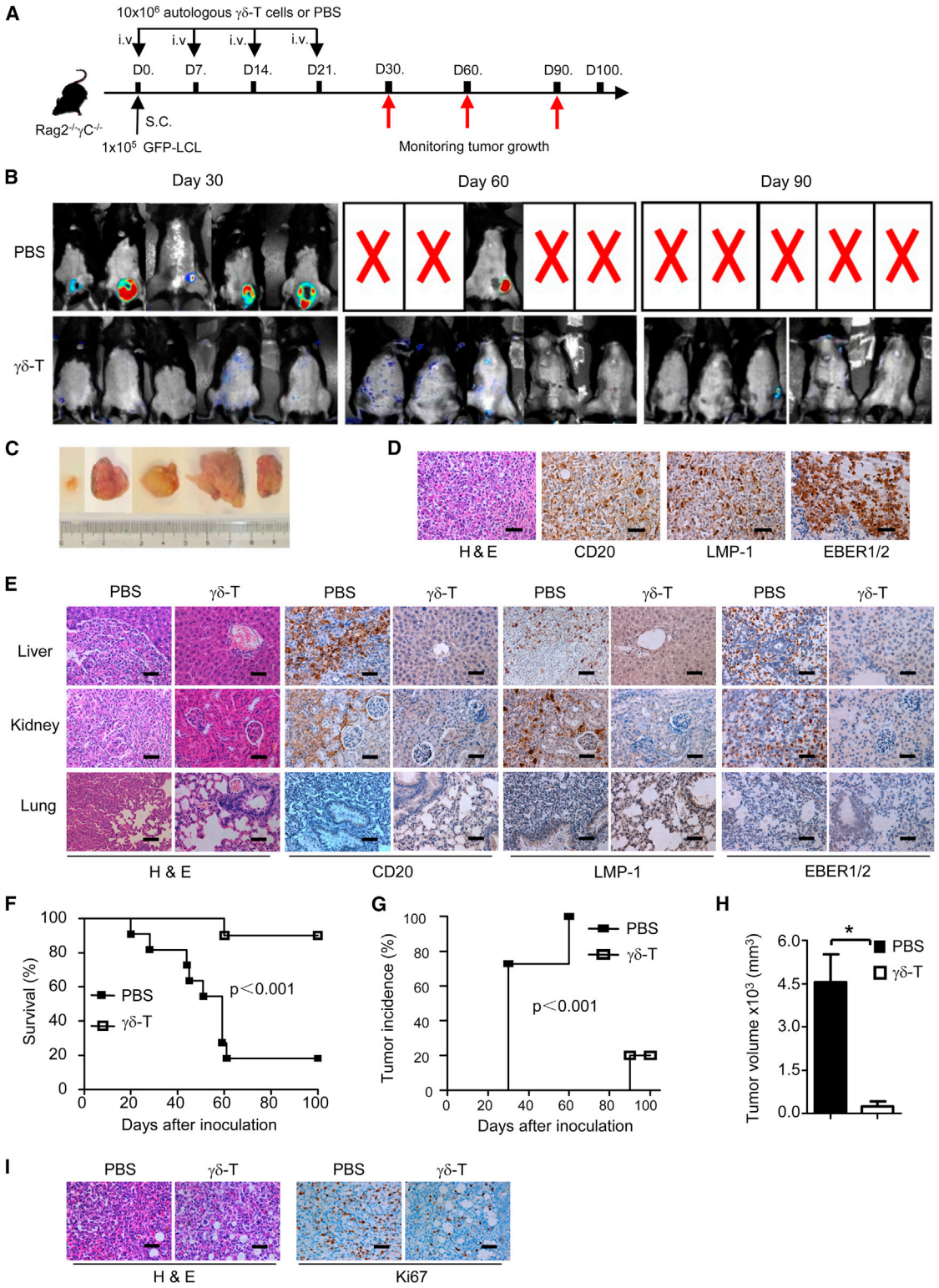

Figure 2. Vγ9Vδ2-T Cells Prevent EBV-LPD in Rag2$^{-/-}$γc$^{-/-}$ Mice

(A) Protocol of establishment of EBV-LPD mice model and evaluation of the antitumor activity of Vγ9Vδ2-T cells in vivo. Rag2$^{-/-}$γc$^{-/-}$ mice were inoculated s.c. with EGFP-expressing EBV-LCL. The PAM-expanded autologous Vγ9Vδ2-T cells were adoptively transferred i.v. into Rag2$^{-/-}$γc$^{-/-}$ mice after inoculation with EBV-LCLs at days 0, 7, 14, and 21. The mice treated with an equivalent volume of PBS were the control group. The subcutaneous tumors were monitored with in vivo imagine system at indicated time.

(B) Whole body fluorescence images in mice treated with PAM-expanded Vγ9Vδ2-T cells or PBS (n = 5 per group) are shown (X = death).

(legend continued on next page)

after 90 days of EBV-LCL inoculation (Figure 2G). After adoptive transfer of Vγ9Vδ2-T cells, these cells could persist for up to 98 days in the peripheral blood in the EBV-LCL-grafted mice (Figure S2). Histological and immunophenotypic analysis of CD20, LPM1, and EBER-1/2 expression showed no evidence of tumor metastases in liver, kidney, and lung at autopsy in Vγ9Vδ2-T cells-treated mice after 100 days after EBV-LCL inoculation except in one mouse that died at day 60 (Figure 2E). Importantly, the volume of subcutaneous tumors in mice receiving Vγ9Vδ2-T cells was significantly reduced when compared to that in PBS-treated mice (Figure 2H). Histological and immunophenotypic analysis of the residual tumors further showed that the B cell lymphomas had fewer Ki67-positive cells in mice receiving Vγ9Vδ2-T cells than that in PBS-treated mice (Figure 2I), indicating the residual tumor cells in Vγ9Vδ2-T cell-treated mice had lower proliferative capacity than that in PBS-treated mice. These data demonstrated that pamidronate-expanded Vγ9Vδ2-T cells alone can effectively prevent EBV-LPD in $Rag2^{-/-}\gamma c^{-/-}$ mice.

Vγ9Vδ2-T Cells Induce the Regression of EBV-LPD in Tumor-Bearing $Rag2^{-/-}\gamma c^{-/-}$ Mice

To determine whether Vγ9Vδ2 T cells had therapeutic effect on EBV-LPD in mice, EGFP-expressing EBV-LCL (0.1×10^6/mouse) were inoculated into $Rag2^{-/-}\gamma c^{-/-}$ mice s.c. (Figure 3A). Twenty-one days later, large subcutaneous tumors (medium surface area, 137 mm^2) had developed in all the mice as detected with in vivo imaging (Figures 3B and 3C). Then half of these tumor-bearing mice were adoptively transferred with highly purified pamidronate-expanded autologous Vγ9Vδ2-T cells (10×10^6 cells/mouse) i.v. at days 21, 28, 35, and 42, and another half of these tumor-bearing mice were treated with PBS as the control (Figure 3A). PBS-treated mice had subcutaneous tumor with progressive growth and extension to the abdominal cavity, liver, and kidney (data not shown), ultimately causing death within 43 days after EBV-LCL inoculation (Figures 3C–3E). In contrast, Vγ9Vδ2-T cell treatment constrained tumor growth, and only one of six mice died at day 107 after EBV-LCL inoculation (Figures 3C and 3D). The other five of six Vγ9Vδ2-T cell-treated mice were still alive more than 170 days after EBV-LCL inoculation (Figure 3D). In addition, Vγ9Vδ2-T cell treatment significantly reduced the volume of the subcutaneous tumors in these five mice (Figures 3C and 3E). At day 170, the surviving five mice were killed and full necropsies performed, and no evidence of tumor metastasis in other organs was found in these surviving mice. In contrast to the intact B cell lymphomas with numerous Ki67-positive cells in PBS-treated mice, histological and immunophenotypic analysis showed large areas of necrosis with calcification and interlaced fibrous tissue and scarce Ki67-positive cells in some residual tumors from Vγ9Vδ2-T cell-treated mice (Figure 3F). These results indicated that pamidronate-expanded Vγ9Vδ2-T cells can induce the regression of EBV-LPD in $Rag2^{-/-}\gamma c^{-/-}$ mice.

Vγ9Vδ2-T Cells Preferentially Home to Subcutaneous Tumor Sites

To evaluate the homing of Vγ9Vδ2-T cells to subcutaneous tumor site, highly purified pamidronate-expanded autologous Vγ9Vδ2-T cells were labeled with a lipophilic dye (DiR), and then injected i.v. into tumor-bearing mice established with EGFP-expressing EBV-LCL. In vivo imaging showed that DiR-labeled Vγ9Vδ2-T cells migrated to the tumor sites from 12 hr after injection and accumulated to a peak level around the tumor sites at 72 hr after injection of Vγ9Vδ2-T cells (Figures 4A and 4B). Confocal fluorescence microscope analysis in tumor sections revealed that Vγ9Vδ2-T cells infiltrated tumors 12 hr after injection (Figure 4C). These data demonstrated that Vγ9Vδ2-T cells can preferentially migrate to subcutaneous tumor sites in mice.

To determine the mechanisms related to the migration of Vγ9Vδ2-T cells, chemokine production in EBV-LCL and chemokine receptor expression in Vγ9Vδ2-T cells were examined. EBV-LCL secreted relatively high levels of CCR5 ligands, that is, macrophage inflammatory protein (MIP)-1α (CCL3), MIP-1β (CCL4), and RANTES (CCL5), but only little or no other chemokines (monocyte chemotactic protein 1, interleukin-8, granulocyte-colony-stimulating factor, monokine induced by gamma-interferon, and interferon gamma-induced protein 10; Figure 4D). Most Vγ9Vδ2-T cells expressed CCR5 (Figure 4E). The migration induced by supernatant from EBV-LCL was abrogated by CCR5 neutralizing antibody in a transwell chemotaxis assay (Figure 4F). In vivo imaging further showed that the migration of Vγ9Vδ2-T cells to tumor sites was significantly prevented when the CCR5 was blocked by its neutralizing antibody (Figures 4E, 4G, and 4H). These results demonstrated that the migration of Vγ9Vδ2-T cells to tumor sites was mainly mediated by CCR5 and its ligands.

Pamidronate Controls the Development of EBV-LPD in Humanized Mice

Previously we had demonstrated that pamidronate could selectively expand human Vγ9Vδ2-T cells, but had no such effect on any other cell subset, such as CD4, CD8, B, or NK cells in vitro and in humanized mice (Tu et al., 2011). We then investigated whether pamidronate could control EBV-LPD in humanized mice with stable reconstitution of huPBMC by expanding Vγ9Vδ2-T cells in vivo. After inoculation with EBV-LCL (1×10^5/mouse) s.c., humanized mice were injected intraperitoneally (i.p.) with pamidronate (10 mg/kg body weight) at days 0, 7, 14, 21, and 28 after EBV-LCL inoculation (Figure 5A). PBS-treated mice were used as controls. Similar to $Rag2^{-/-}\gamma c^{-/-}$ mice, EBV-LPD with subcutaneous tumors developed in all PBS-treated humanized mice after EBV-LCL inoculation (Figure 5B).

(C) Typical appearance of subcutaneous tumor in $Rag2^{-/-}\gamma c^{-/-}$ mice from PBS-treated group at autopsy.
(D, E, and I) Representative histological analysis, immunohistological stainings for human CD20, LMP1, Ki-67, and in situ hybridization for EBER-1/2 in formalin-fixed paraffin-embedded sections from a tumor (D and I) and liver, kidney and lung in mice treated with PAM-expanded Vγ9Vδ2-T cells or PBS (E). Scale bar represents 100 μm.
(F–H) After treatment with PAM-expanded Vγ9Vδ2-T cells (n = 10) or PBS (n = 11), the survival (F), tumor incidence (G), and tumor volume (mean ± SEM) at autopsy (H) were measured. *$p < 0.05$.
See also Figure S2.

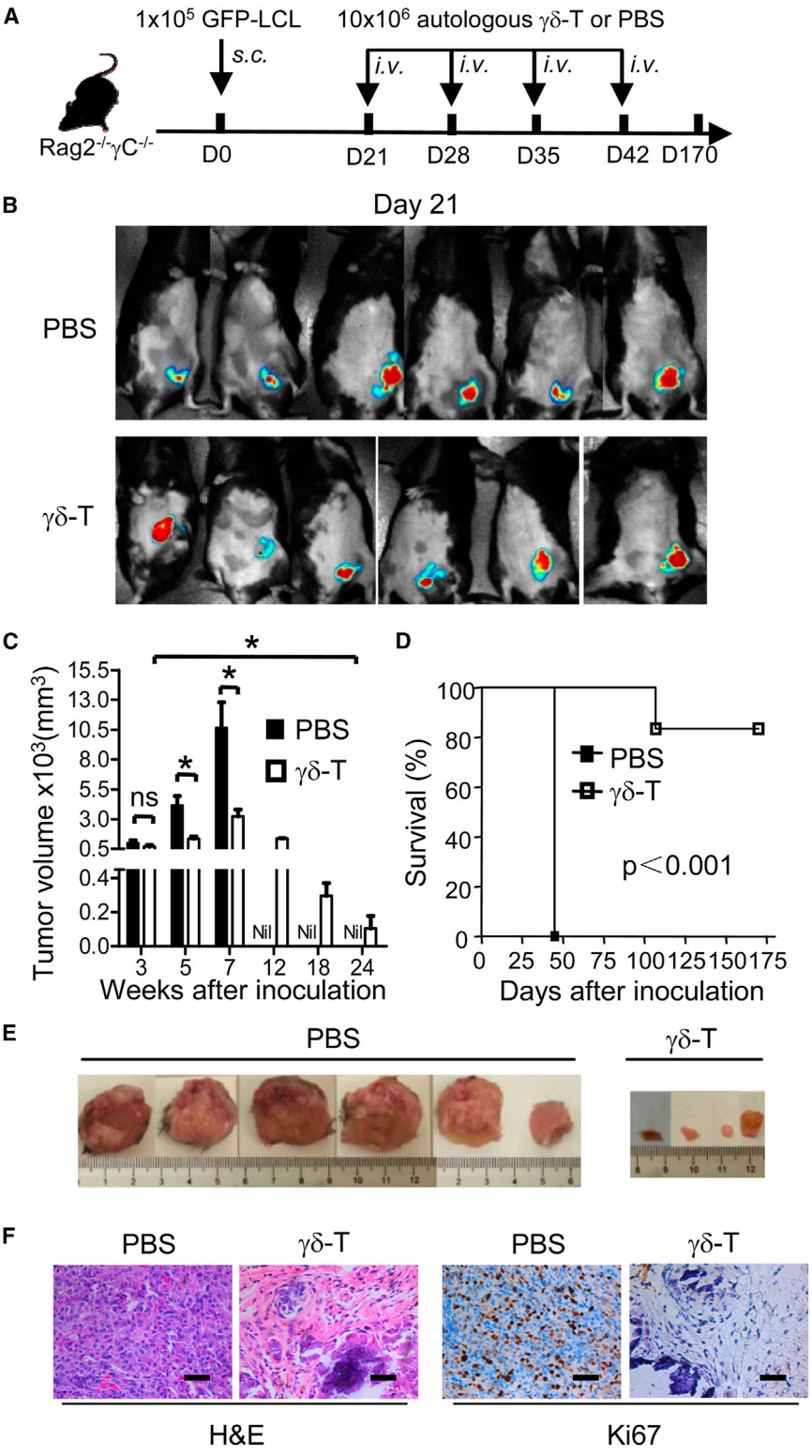

Figure 3. Vγ9Vδ2-T Cells Induce the Regression of EBV-LPD in Tumor-Bearing Rag2$^{-/-}$γc$^{-/-}$ Mice

(A) Protocol for evaluation of the therapeutic effect of Vγ9Vδ2-T cells EBV-LPD in tumor-bearing Rag2$^{-/-}$γc$^{-/-}$ mice. EGFP^{+} EBV-LCL were inoculated into Rag2$^{-/-}$γc$^{-/-}$ mice s.c.. Twenty-one days later, half of these tumor-bearing mice were adoptively transferred with the PAM-expanded autologous Vγ9Vδ2-T cells i.v. at the indicated time and another half of these mice were treated with PBS as the control.

(B) Whole body fluorescence images in mice before treatment with Vγ9Vδ2-T cells or PBS.

(C and D) After treatment with Vγ9Vδ2-T cells (n = 6) or PBS (n = 6), the tumor volume (C) and survival (D) in tumor-bearing Rag2$^{-/-}$γc$^{-/-}$mice were measured at the indicated time. Data are mean ± SEM.

(E) Macroscopic appearance of the tumors in Vγ9Vδ2-T cell and PBS treated mice at autopsy.

(F) Representative histological analysis and immunohistological staining for Ki-67 in formalin-fixed paraffin-embedded sections from tumors in mice treated with PAM-expanded Vγ9Vδ2-T cells or PBS. Scale bar represents 100 μm. ns, no significant difference. *p < 0.05.

These tumor cells were positive for human CD20, LMP1, and EBER-1/2 (Figure 5C). As in Rag2$^{-/-}$γc$^{-/-}$ mice, tumor metastases were found in liver, kidney, and lung in humanized mice (Figure 5D). Due to EBV-LPD, all humanized mice died within 100 days of observation (Figure 5E).

Treatment with pamidronate significantly increased the frequency of Vγ9Vδ2-T cells in the peripheral blood, and the cells could persist for up to 98 days in EBV-LCL-grafted humanized mice (Figure S3). Pamidronate treatment also significantly prolonged the survival of humanized mice (Figure 5E). In the pamidronate treatment group, only one out of eight (12.5%) mice died and three of eight mice (37.5%) had subcutaneous tumor growth within 100 days. Importantly, humanized mice receiving pamidronate treatment had significantly lower tumor incidence and reduced tumor volume, compared with PBS-treated humanized mice (Figures 5F and 5G). At day 100, the surviving seven mice were killed and full necropsies failed to show any evidence of tumor metastasis in other organs (Figure 5D). Histological and immunophenotypic analysis of the residual tumors showed that the B cell lymphomas had fewer Ki67-positive cells in mice receiving Vγ9Vδ2-T cells than that in PBS-treated mice (Figure 5H), indicating the residual tumor cells in Vγ9Vδ2-T cell-treated mice had lower proliferative capacity than that in PBS-treated mice. These data demonstrated that pamidronate can effectively control the development of EBV-LPD in humanized mice.

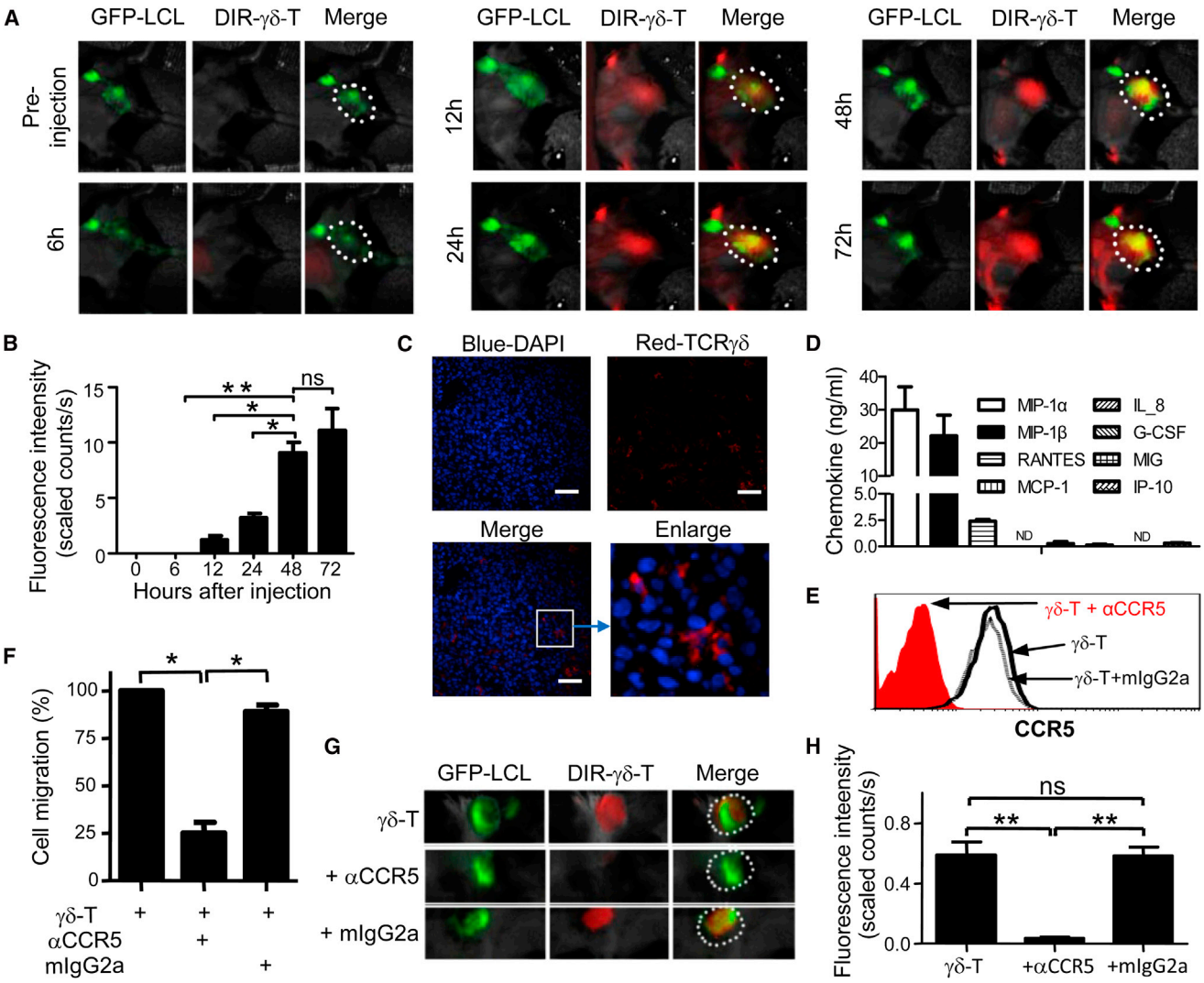

Figure 4. Homing Program of Vγ9Vδ2-T Cells in Tumor-Bearing Rag2$^{-/-}$γc$^{-/-}$ Mice

(A and B) DiR-labeled PAM-expanded Vγ9Vδ22-T cells were adoptively transferred into Rag2$^{-/-}$γc$^{-/-}$ mice with subcutaneous tumors after EGFP^{+} EBV-LCL inoculation. The migration and accumulation of Vγ9Vδ2-T cells (DiR-labeled, red) in the tumor sites (EGFP^{+}, green) were monitored at indicated time after injection (A). The fluorescence intensity of DiR signal was measured in the indicated area with dashed lines (B). Data are means ± SEM.

(C) Infiltrated Vγ9Vδ2-T cells (red) within tumor tissues at 12 hr after adoptive transfer of Vγ9Vδ2-T cells analyzed with a confocal fluorescence microscope. Scale bar represents 100 μm.

(D) The concentrations of chemokines (means ± SEM) in the supernatants from EBV-LCL were measured (n = 4).

(E) The surface expression of CCR5 on Vγ9Vδ2-T cells after treatment with anti-CCR5 blocking antibody (αCCR5) or its isotype control (mouse IgG2a, mIgG2a) for 2 hr is shown.

(F) Vγ9Vδ2-T cells were preincubated with αCCR5, or mIgG2a for 30 min and placed in the upper well. The supernatants from EBV-LCL were added into the lower well. The percentages of cells (means ± SEM) that have migrated from the upper well after 4 hr are shown (n = 4).

(G and H) DiR-labeled PAM-expanded Vγ9Vδ2-T cells were pretreated with αCCR5 or mIgG2a for 2 hr, and then adoptively transferred into EGFP^{+} EBV-LCL subcutaneous tumor-bearing mice. The migration and accumulation of Vγ9Vδ2-T cells (DiR-labeled, red) in the tumor sites (EGFP^{+}, green) were detected at 24 hr after injection (G). The fluorescence intensity of DiR signal was measured in the indicated area with dashed lines (H). Data are means ± SEM. Data represent three to four independent experiments. ns, no significant difference; ND, undetectable. *p < 0.05; **p < 0.01.

Pamidronate Cannot Control EBV-LPD in Humanized Mice without Vγ9Vδ2-T Cells

To further determine whether the control of EBV-LPD by pamidronate was mediated through Vγ9Vδ2-T cells in humanized mice, mice reconstituted with Vγ9Vδ2-T cell-depleted huPBMC were used (Tu et al., 2011). Mice reconstituted with whole huPBMC or Vγ9Vδ2-T cell-depleted huPBMC were inoculated with EBV-LCL s.c. and injected with pamidronate (10 mg/kg body weight) i.p. at days 0, 7, 14, 21, and 28 after EBV-LCL inoculation. Treatment with pamidronate significantly prolonged survival (Figure 6A), reduced tumor occurrence (Figure 6B), and decreased tumor volume (Figure 6C) in humanized mice with whole huPBMC. In contrast, pamidronate had no such effects in humanized mice reconstituted with Vγ9Vδ2-T cell-depleted

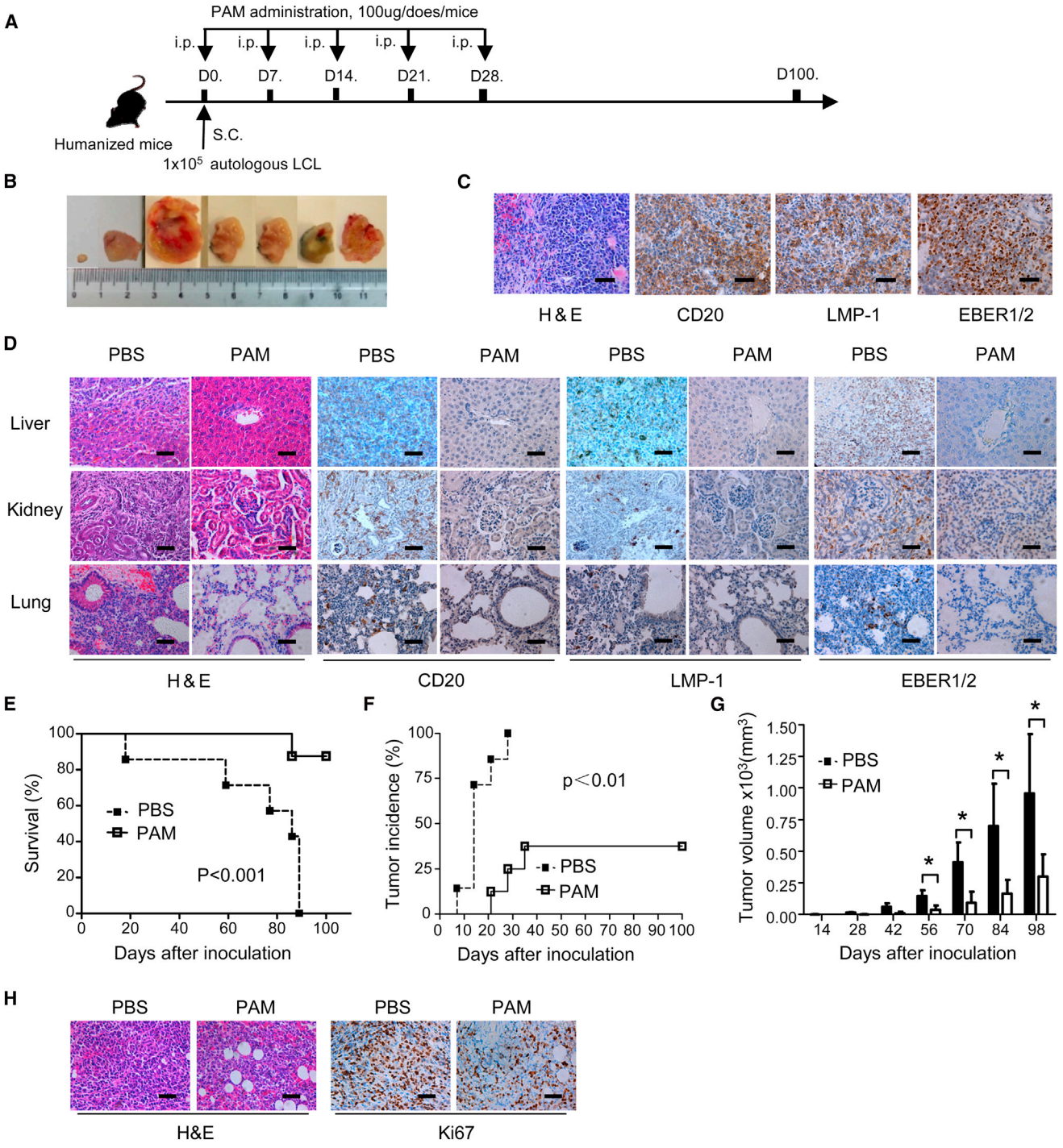

Figure 5. Pamidronate Controls the Development of EBV-LPD in Humanized Mice

(A) Protocol for the control of EBV-LPD by pamidronate (PAM) in humanized mice. Humanized mice were treated with PAM or PBS at days 0, 7, 14, 21, and 28 after inoculation of EBV-LCL.

(B) Typical appearance of subcutaneous tumor in humanized mice from PBS-treated group at autopsy.

(C, D, and H) Representative histological analysis and immunohistological staining for human CD20, LMP1, and Ki-67, and in situ hybridization for EBER-1/2 in formalin-fixed paraffin-embedded sections from a tumor (C and H) and liver, kidney, and lung in humanized mice treated with PAM or PBS (D). Scale bar represents 100 μm.

(E–G) After treatment with PAM (n = 8) or PBS (n = 7), the survival (E), tumor incidence (F), and tumor volume (G) were measured at the indicated time. Data are means ± SEM. *p < 0.05.

See also Figure S3.

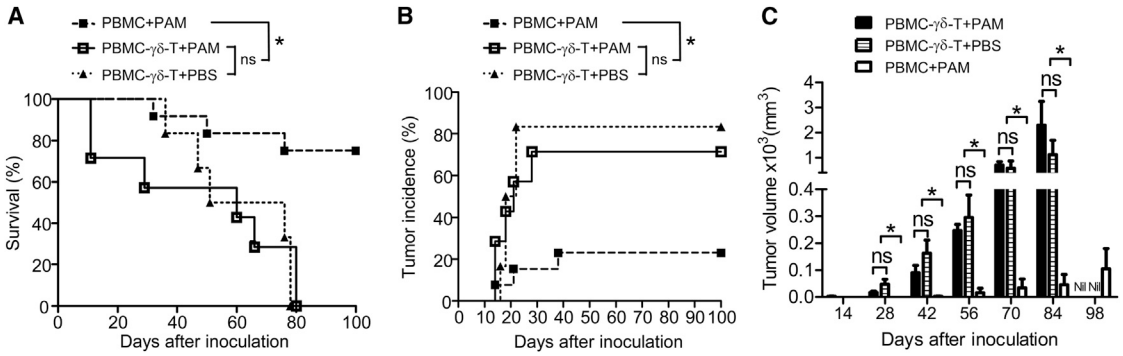

Figure 6. Pamidronate Cannot Control EBV-LPD in Humanized Mice without Vγ9Vδ2-T Cells

(A–C) Vγ9Vδ2-T cell-depleted huPBMC were obtained after double depletions of Vδ2-T cells by positive selection with magnetic microbeads. Rag2$^{-/-}$γc$^{-/-}$ mice were transplanted with whole huPBMC or Vγ9Vδ2-T cell-depleted huPBMC from the same healthy human donor. In contrast to the mice reconstituted with whole huPBMC, there were scanty or no human Vγ9Vδ2-T cells in the mice reconstituted with Vγ9Vδ2-T cell-depleted huPBMC. Humanized mice reconstituted with whole huPBMC (PBMC) or Vγ9Vδ2-T cell-depleted huPBMC (PBMC-γδ-T) were inoculated with EBV-LCL and treated with pamidronate or PBS according to the protocol showed in Figure 5A. The survival (A), tumor incidence (B), and tumor volume (C) in humanized mice (PBMC + PAM, n = 12; PBMC-γδ-T + PAM, n = 7; PBMC-γδ-T + PBS, n = 6) are shown. Data are means ± SEM. ns, not significant. *p < 0.05.

huPBMC. These results demonstrated that the control of EBV-LPD in humanized mice by pamidronate is mainly mediated by a Vγ9Vδ2-T cell-dependent mechanism.

DISCUSSION

Immunodeficient mice are widely used as a preclinical model of EBV studies because lethal human EBV-LPD can develop rapidly in these mice inoculated with human EBV-LCL, with characteristics similar to those arising in immunocompromised humans (Funakoshi et al., 1994; Lacerda et al., 1996). By inoculation of human EBV-LCL in immunodeficient Rag2$^{-/-}$γc$^{-/-}$ mice, we established lethal EBV-LPD in these mice. Using this model, we demonstrated that adoptive transfer of pamidronate-expanded human Vγ9Vδ2-T cells alone not only effectively prevented EBV-LPD in Rag2$^{-/-}$γc$^{-/-}$ mice, but also induced the regression of EBV-LPD in EBV-induced tumor-bearing Rag2$^{-/-}$γc$^{-/-}$ mice. The lack of a human immune system in Rag2$^{-/-}$γc$^{-/-}$ mice hampers assessment of the pathogenesis, prevention, and treatment of EBV-LPD, but this can be circumvented by reconstitution with huPBMC or CD34^{+} stem cells (Lim et al., 2007; Ma et al., 2011). Recently we had established humanized mice with functional human immune system by reconstitution of huPBMC in Rag2$^{-/-}$γc$^{-/-}$ mice (Tu et al., 2011; Zheng et al., 2013b). These humanized mice contain functional human T and B cells, including a similar percentage of Vγ9Vδ2-T cells in peripheral blood as seen in humans (Tu et al., 2011; Zheng et al., 2013b). In this study, we further induced lethal EBV-LPD in these humanized mice by inoculation of human EBV-LCL and showed in this model that pamidronate treatment inhibited development of EBV-LPD through selective activation and expansion of Vγ9Vδ2-T cells in vivo.

Although it has been showed that human γδ-T cells have antiviral and antitumor activities (Bonneville et al., 2010; Kabelitz et al., 2007), data supporting their reactivity toward EBV are still scarce (Kong et al., 2009; Kotsiopriftis et al., 2005). Whereas one study described in vitro recognition of EBV-LCL by Vδ1^{+} γδ-T cell clones (Orsini et al., 1994), EBV-LCL are classically used as negative controls in in vitro cytotoxicity assays using Vγ9Vδ2-T cells. Accordingly, we confirmed the lack of EBV-LCL killing by pamidronate-expanded Vγ9Vδ2-T cells sorted by negative selection but unexpectedly unveiled significant cytotoxicity against EBV-LCL by the same cell subset after positive sorting using anti-TCR monoclonal antibodies (mAb). This suggests that recently activated Vγ9Vδ2-T cells can trigger the cytotoxic activity against EBV-LCL soon after TCR engagement. Our results further indicate that this process requires cell-cell contact and involves engagement of NKG2D on Vγ9Vδ2-T cells with MICA/B expressed on EBV-LCL. Indeed, we also found that the immobilized MICA/B enhanced Vγ9Vδ2-T cell activation, granule exocytosis, and cytotoxic activity. Importantly, upon the immobilized MICA/B stimulation, the levels of the granule exocytosis and cytotoxicity of Vγ9Vδ2-T cells sorted by negative selection were much lower than those in the same cells after positive sorting using anti-TCR mAb. Therefore, both TCR-γ/δ and NKG2D are required for the recognition of Vγ9Vδ2-T cells and TCR-γ/δ engagement is essential for triggering their cytotoxic activity against EBV-LCL.

In line with our previous results using influenza virus-infected cells (Qin et al., 2009), we also found that the cytotoxic activity of Vγ9Vδ2-T cells against EBV-LCL involved engagement of the death-inducing Fas receptor and release of cytotoxic effector molecules, such as perforin and granzyme. We further demonstrated that interaction of another death-inducing receptor DR5 expressed by EBV-LCL with TRAIL expressed on Vγ9Vδ2-T cells also enhanced Vγ9Vδ2-T cell-mediated EBV-LCL killing. Importantly, these pamidronate-expanded Vγ9Vδ2-T cells could migrate to tumor site and infiltrate into tumor tissues in vivo, thus contributing to the control of EBV-LPD in mice. Consistent with our previous findings in chemotaxis assay using influenza virus-infected cells (Qin et al., 2011), using both transwell chemotaxis and in vivo imaging assays, here we further showed that the migration of Vγ9Vδ2-T cells to tumor sites was mainly mediated by CCR5 and its ligands. Taken together, our results indicate that pamidronate-expanded Vγ9Vδ2-T cells can control EBV-LPD by killing EBV-LCL.

Our previous data showed that pamidronate-expanded Vγ9Vδ2-T cells can produce a large amount of interferon gamma (IFN-γ; Qin et al., 2011). One study also demonstrated that IFN-γ secreted from NK cells can delay latent EBV antigen expression, thus resulting in decreased EBV-induced B cell proliferation (Strowig et al., 2008). We also found the decreased proliferative capacity of tumor cells in Vγ9Vδ2-T cell- and pamidronate-treated mice, compared with that in control mice. Therefore, besides their direct killing, Vγ9Vδ2-T cells might also contribute to the prevention of the metastases by inhibiting the proliferation of EBV-LCL through their secreted IFN-γ.

We and others previously showed pamidronate-induced expansion of Vγ9Vδ2-T cells, but not other T cell subsets, both in vitro and in humanized mice (Das et al., 2001; Kunzmann et al., 1999; Sicard et al., 2005; Tu et al., 2011). Although non-Vγ9Vδ2 γδ T cells could be also activated by pamidronate, the frequencies of $CD69^+$, $perforin^+$, and granzyme B^+ cells in non-Vγ9Vδ2 γδ T cells were significantly lower than those in Vγ9Vδ2-T cells (Tu et al., 2011). Indeed, our adoptive transfer experiments in $Rag2^{-/-}\gamma c^{-/-}$ mice further showed that pamidronate-expanded Vγ9Vδ2-T cells readily controlled EBV-LPD in vivo without help from other human and murine T, B, and NK cells, which are absent in $Rag2^{-/-}\gamma c^{-/-}$ mice. Importantly, pamidronate effectively controlled the development of EBV-LPD in humanized mice reconstituted with whole huPBMC, but had no such beneficial effects in mice reconstituted with Vγ9Vδ2-T cell-depleted huPBMC. In addition, pamidronate did not show any cytotoxic activity against EBV-LCL. Therefore, this indicates that control of EBV-LPD by pamidronate in humanized mice is mainly mediated by Vγ9Vδ2-T cells.

As in humans, Vγ9Vδ2-T cells make up a small percentage of lymphocytes in humanized mice (Tu et al., 2011). The antitumor activity of Vγ9Vδ2-T cells depends on both Vγ9Vδ2-T cell frequency and degree of activation (Bonneville and Scotet, 2006). Therefore, we could not observe a difference in disease severity between mice reconstituted with whole huPBMC and Vγ9Vδ2-T cell-depleted huPBMC. Indeed, our in vitro results also showed that EBV-LCL alone could not efficiently expand Vγ9Vδ2-T cells in EBV-seropositive donors. It was only in the presence of pamidronate that Vγ9Vδ2-T cells could be expanded and also induced to express sufficient levels of EBV-LCL recognition receptors as well as cytotoxic molecules to control the growth of EBV-LCL.

By contrast with results of adoptive transfer of EBV-specific CTL that lead to durable eradications of the tumors (Kanakry and Ambinder, 2013; Khanna et al., 1999; Leen et al., 2007; Rooney et al., 1995), we showed in some mice that Vγ9Vδ2-T cell-based therapy could not completely eradicate the primary tumors. The variations in frequency and activation of Vγ9Vδ2-T cells in different mice might account for this. Thus, it is important to adjust the dose of pamidronate in real-time according to results by monitoring the therapeutic effects and frequency of Vγ9Vδ2-T cells. Nevertheless, the strategy proposed in this study by using pamidronate to control EBV-LPD through boosting Vγ9Vδ2-T cell immunity in vivo has an obvious advantage because it may avoid the complicated procedures for generation of EBV-specific CTL in vitro.

In summary, our study demonstrated that pamidronate-expanded Vγ9Vδ2-T cells can directly kill the EBV-LCL in vitro and in vivo, and pamidronate can control EBV-LPD in humanized mice through a Vγ9Vδ2-T cell dependent mechanism. Our study provides a strong preclinical proof of principle for a therapeutic approach using pamidronate to boost human Vγ9Vδ2-T cell immunity against EBV-LPD. Pamidronate is commonly used clinically for the treatment of osteoporosis and Paget disease, and the use of a human equivalent dose of pamidronate can effectively control EBV-LPD in humanized mice, suggesting rapid translation to human clinical trials. This "new application of an old drug" potentially offers a safe and readily available option for the treatment of EBV-LPD.

EXPERIMENTAL PROCEDURES

Establishment of EBV-LCL In Vitro

huPBMC were isolated from buffy coats of EBV-seropositive health donors after informed consents were obtained. The research protocol was approved by the Institutional Review Board of the University of Hong Kong/Hospital Authority Hong Kong West Cluster. EBV-LCL were established as described before (Lacerda et al., 1996). Briefly, huPBMC were infected with supernatants from the EBV-secreting cell line B95-8 or B95.8EBfaV-GFP, carrying an enhanced green fluorescent protein (EGFP, kindly provided by Diane Hayward, Johns Hopkins University, Baltimore; Speck and Longnecker, 1999), and then cultured in the RPMI 1640 supplemented with 15% heat-inactivated fetal bovine serum (FBS).

Expansion and Purification of Vγ9Vδ2-T Cells In Vitro

Pamidronate-expanded Vγ9Vδ2-T cells were generated as described before (Tu et al., 2011). Briefly, huPBMC were cultured in RPMI 1640 medium supplemented with 10% FBS. Pamidronate was added at day 0 and day 3 to a final concentration 9 μg/ml. Recombinant human interleukin-2 (Invitrogen) was added to a final concentration of 500 UI/ml every third day from day 3. After 14 days of culture, the Vγ9Vδ2-T cells were purified by positive selection or negative selection with anti-TCRγ/δ MicroBead or $TCR\gamma/\delta^+$ T cell isolation kit (Miltenyi Biotec). The purity of Vγ9Vδ2-T cells, as determined with flow cytometry with anti-CD3 and anti-Vδ2 mAbs, was consistently >97%.

Establishment of EBV-LPD Model and Treatment of EBV-LPD in Humanized and $Rag2^{-/-}\gamma c^{-/-}$ Mice

All animal studies were approved and performed in compliance with the guidelines for the use of experimental animals by the Committee on the Use of Live Animals in the Teaching and Research, the University of Hong Kong. Humanized mice were generated in 4- to 5-week-old male or female $Rag2^{-/-}\gamma c^{-/-}$ mice by reconstitution of EBV seropositive whole huPBMC or Vγ9Vδ2-T cell-depleted huPBMC as we described before (Tu et al., 2011). After 4 weeks of huPBMC transplantation, mice were successfully engrafted and became stable with functional human immune system (Tu et al., 2011), and then used for establishment of EBV-LPD. Humanized mice or 6- to 8-week-old $Rag2^{-/-}\gamma c^{-/-}$ mice were inoculated s.c. with EBV-LCL or EGFP-expressing EBV-LCL (0.1×10^6/mouse). For $Rag2^{-/-}\gamma c^{-/-}$ mice, pamidronate-expanded autologous Vγ9Vδ2-T cells (10×10^6/mouse) in 200 μl of PBS were adoptively transferred i.v. into mice after inoculation with EBV-LCLs at indicated time. For humanized mice, a human equivalent dose of PAM (10 mg/kg body weight; Pamisol; Hospira NZ) was injected i.p. at indicated time. The mice treated with an equivalent volume of PBS were used as controls. The signs of disease (loss of activity, weight loss, ruffled hair, palpable tumors, and ascites) and survival of mice were monitored. Mice with more than 17 mm diameter subcutaneous tumor were killed and counted as dying. Otherwise, mice were followed for 100 or 170 days and then killed. All mice were examined for postmortem evidence of tumor. The tumors and organs were collected for histology and immunohistochemistry assays.

In Vivo Tracking with DiR-Labeled Vγ9Vδ2-T Cells

Vγ9Vδ2-T cells were stained with DiR (Invitrogen), and then these DiR-labeled cells were adoptively transferred intravenously into subcutaneous EGFP-EBV tumor-bearing mice. The migration and accumulation of Vγ9Vδ2-T cells were

depicted and analyzed with a TM 2 in vivo imaging system (CRI Maestro) at the indicated time. After 12 hr, some mice were killed, and tumor sections were snap-frozen and stained with anti-human TCR γ/δ mAb (5 μg/ml; B-1, Biolegend). These cryostat sections were analyzed with a Confocal Laser Scanning Microscope (LSM 700, Carl Zeiss).

Chemotaxis Assay

The in vitro migration of purified Vγ9Vδ2-T cells was assessed in a transwell system (24-well; pore size, 5.0 μm; polycarbonate membranes; Corning-Costar) as we described before (Qin et al., 2011). Briefly, supernatants from EBV-LCL after 24 hr of culture in RPMI 1640 medium were collected, and loaded in the lower compartment. A total of 100 μl of autologous Vγ9Vδ2-T cells (4×10^5) in serum-free RPMI 1640 medium was added to the upper compartment of the chamber. After 4 hr, the cells that had migrated through the membrane to the lower compartment were collected and counted by flow cytometry with counting beads. The migration of Vγ9Vδ2-T cells in control group (γδ-T cells alone) was set to 100% and the results obtained from other treatment group or isotype control group were expressed as a percentage of the control. In blocking experiments, Vγ9Vδ2-T cells were preincubated for 30 min with either anti-CCR5 mAb (20 μg/ml; clone 2D7, BD) or isotype control mouse IgG2a (20 μg/ml) mAb.

Cytotoxic Assay

The death of EBV-LCL (target) was analyzed with flow cytometry after 4–6 hr of coculture with autologous Vγ9Vδ2-T cells (effector) at different E:T ratios. In some experiments, a transwell system (24 wells; pore size, 0.4 um; Corning-Costar) was used to separate Vγ9Vδ2-T cells from EBV-LCL as we did before (Qin et al., 2009). In some experiments, neutralization antibodies anti-NKG2D (10 μg/ml; 149810, R&D System), anti-Fas-L (10 μg/ml; NOK-1, Biolegend), anti-TRAIL (10 μg/ml; RIK-2, Biolegend), and isotype control mouse IgG1 (10 μg/ml) were used for blocking NKG2D-, FasL-, and TRAIL-mediated pathways (Qin et al., 2009). For MICA/B immobilization, 24-well plates were coated with recombinant MICA/B proteins (Sino Biological) overnight. The plates were carefully washed to remove the unbound protein and then incubated with Vγ9Vδ2-T cells for 6 hr. For blocking perforin and granzyme B, the perforin inhibitor concanamycin A (1 μg/ml; Sigma) and the granzyme B inactivator Bcl-2 (1 μg/ml; R&D Systems) were used as we did before (Qin et al., 2009). Cytotoxicity was analyzed with flow cytometry and calculated as the percentage of inhibition relative to that in controls. Cells were stained with anti-CD3 to identify Vγ9Vδ2-T cells and propidium iodide (PI) was used to identify dead cells. The death of EBV-LCL was shown as the percentage of PI^+ cells in the $CD3^-$ population (Qin et al., 2009).

Histopathology and Immunohistochemistry

Samples of tumors and organs to be analyzed were fixed in 10% formalin, embedded in paraffin, sectioned, and stained with hematoxylin and eosin. To investigate the presence of EBV, tissues were stained with mouse anti-EBV LMP1 (ab58938, Abcam) and the presence of human B cells in tissues was assessed using rabbit anti-human CD20 (EP459Y, Abcam) with immunoperoxidase techniques. The proliferative rate of cells and the aggressive nature of lymphomas were indicated by histological staining of Ki67 (ab136912, Abcam). Demonstration of immunostaining was performed with a diaminobenzidine detection kit (DAB-0031, Maixin) and the sections were counterstained with hematoxylin.

In Situ Hybridization

In situ hybridization of paraffin sections from tumors and mouse organs to detect EB-encoded small RNAs type 1 and 2 (EBER-1/2) was performed using a DIG-HRP REMBRANDT EBER ISH kit (Tzartos et al., 2012; A500K.9901, Panpath) according to the manufacturer's protocol.

Flow Cytometric Analysis

Cells were stained for surface markers with the following antibodies: anti-CD3 (HIT3a), anti-TCR Vδ2 (B6), anti-CD69 (FN50), anti-NKG2D (1D11), anti-Fas (DX2), anti-CD107a (H4A3), anti-FasL (NOK-1), anti-TRAIL (RIK-2), anti-MICA/B (6D4), anti-DR4 (DJR1), anti-DR5 (DJR2-4), and anti-CCR5 (2D7). For the intracellular staining, cells were fixed, permeabilized, and then stained with anti-perforin (δG9) and anti-granzyme B (GB11) antibodies (BD) or their relevant isotype controls as described previously (Qin et al., 2009; Tu et al., 2011). All samples were acquired with a FACSLSR II (BD) and analyzed with FlowJo software (Tree Star).

Flowcytomix Assay

The concentrations of chemokines in the supernatants from EBV-LCL culture were detected and analyzed with human chemokine assay kits (Bender MedSystems) as described before (Zheng et al., 2013b).

Statistical Analysis

Data are expressed as means ± SEM. The difference in cell death and viral copy for in vitro experiments and intensity of florescence, tumor incidence, and tumor size between PBS and treatment groups were analyzed with impaired two-tailed Student's t test. The p value of difference for survival was determined with Kaplan-Meier log-rank test; $p < 0.05$ was considered to be significant.

SUPPLEMENTAL INFORMATION

Supplemental Information includes three figures and can be found with this article online at http://dx.doi.org/10.1016/j.ccr.2014.07.026.

AUTHOR CONTRIBUTIONS

W.T. conceived and designed the study, interpreted the results and wrote the manuscript; Z.X. and Y.L. designed experiments, and analyzed and interpreted the results with assistance from J.Z., M.L., A.L., Y.G., H.H, L.K.T., G.C.F.C., Y.Y., H.C., G.S.W.T., and Y. L. L.; G.C.F.C., M.B., and Y.L.L. edited the manuscript.

ACKNOWLEDGMENTS

This work was supported in part by General Research Fund, Research Grants Council of Hong Kong (HKU 781211M), the Area of Excellence program supported by the University Grants Committee of the Hong Kong SAR, China (AoE/M-12/06 and AoE/M-06/08).

Received: February 14, 2014
Revised: May 4, 2014
Accepted: July 28, 2014
Published: September 11, 2014

REFERENCES

Alexander, A.A., Maniar, A., Cummings, J.S., Hebbeler, A.M., Schulze, D.H., Gastman, B.R., Pauza, C.D., Strome, S.E., and Chapoval, A.I. (2008). Isopentenyl pyrophosphate-activated CD56+ gammadelta T lymphocytes display potent antitumor activity toward human squamous cell carcinoma. Clin. Cancer Res. *14*, 4232–4240.

Beetz, S., Wesch, D., Marischen, L., Welte, S., Oberg, H.H., and Kabelitz, D. (2008). Innate immune functions of human gammadelta T cells. Immunobiology *213*, 173–182.

Bonneville, M., and Scotet, E. (2006). Human Vgamma9Vdelta2 T cells: promising new leads for immunotherapy of infections and tumors. Curr. Opin. Immunol. *18*, 539–546.

Bonneville, M., O'Brien, R.L., and Born, W.K. (2010). Gammadelta T cell effector functions: a blend of innate programming and acquired plasticity. Nat. Rev. Immunol. *10*, 467–478.

Born, W.K., Reardon, C.L., and O'Brien, R.L. (2006). The function of gammadelta T cells in innate immunity. Curr. Opin. Immunol. *18*, 31–38.

Carding, S.R., and Egan, P.J. (2002). Gammadelta T cells: functional plasticity and heterogeneity. Nat. Rev. Immunol. *2*, 336–345.

Cohen, J.I. (2000). Epstein-Barr virus infection. N. Engl. J. Med. *343*, 481–492.

Das, H., Wang, L., Kamath, A., and Bukowski, J.F. (2001). Vgamma2Vdelta2 T-cell receptor-mediated recognition of aminobisphosphonates. Blood *98*, 1616–1618.

Fournié, J.J., Sicard, H., Poupot, M., Bezombes, C., Blanc, A., Romagné, F., Ysebaert, L., and Laurent, G. (2013). What lessons can be learned from γδ T cell-based cancer immunotherapy trials? Cell. Mol. Immunol. *10*, 35–41.

Funakoshi, S., Longo, D.L., Beckwith, M., Conley, D.K., Tsarfaty, G., Tsarfaty, I., Armitage, R.J., Fanslow, W.C., Spriggs, M.K., and Murphy, W.J. (1994). Inhibition of human B-cell lymphoma growth by CD40 stimulation. Blood *83*, 2787–2794.

Heslop, H.E., Slobod, K.S., Pule, M.A., Hale, G.A., Rousseau, A., Smith, C.A., Bollard, C.M., Liu, H., Wu, M.F., Rochester, R.J., et al. (2010). Long-term outcome of EBV-specific T-cell infusions to prevent or treat EBV-related lymphoproliferative disease in transplant recipients. Blood *115*, 925–935.

Kabelitz, D., Wesch, D., and He, W. (2007). Perspectives of gammadelta T cells in tumor immunology. Cancer Res. *67*, 5–8.

Kanakry, J.A., and Ambinder, R.F. (2013). EBV-related lymphomas: new approaches to treatment. Curr. Treat. Options Oncol. *14*, 224–236.

Khanna, R., Bell, S., Sherritt, M., Galbraith, A., Burrows, S.R., Rafter, L., Clarke, B., Slaughter, R., Falk, M.C., Douglass, J., et al. (1999). Activation and adoptive transfer of Epstein-Barr virus-specific cytotoxic T cells in solid organ transplant patients with posttransplant lymphoproliferative disease. Proc. Natl. Acad. Sci. USA *96*, 10391–10396.

Khanna, R., Moss, D., and Gandhi, M. (2005). Technology insight: Applications of emerging immunotherapeutic strategies for Epstein-Barr virus-associated malignancies. Nat. Clin. Pract. Oncol. *2*, 138–149.

Kong, Y., Cao, W., Xi, X., Ma, C., Cui, L., and He, W. (2009). The NKG2D ligand ULBP4 binds to TCRgamma9/delta2 and induces cytotoxicity to tumor cells through both TCRgammadelta and NKG2D. Blood *114*, 310–317.

Kotsiopriftis, M., Tanner, J.E., and Alfieri, C. (2005). Heat shock protein 90 expression in Epstein-Barr virus-infected B cells promotes gammadelta T-cell proliferation in vitro. J. Virol. *79*, 7255–7261.

Kunzmann, V., Bauer, E., and Wilhelm, M. (1999). Gamma/delta T-cell stimulation by pamidronate. N. Engl. J. Med. *340*, 737–738.

Lacerda, J.F., Ladanyi, M., Louie, D.C., Fernandez, J.M., Papadopoulos, E.B., and O'Reilly, R.J. (1996). Human Epstein-Barr virus (EBV)-specific cytotoxic T lymphocytes home preferentially to and induce selective regressions of autologous EBV-induced B cell lymphoproliferations in xenografted C.B-17 scid/scid mice. J. Exp. Med. *183*, 1215–1228.

Leen, A.M., Rooney, C.M., and Foster, A.E. (2007). Improving T cell therapy for cancer. Annu. Rev. Immunol. *25*, 243–265.

Li, H., Xiang, Z., Feng, T., Li, J., Liu, Y., Fan, Y., Lu, Q., Yin, Z., Yu, M., Shen, C., and Tu, W. (2013). Human Vγ9Vδ2-T cells efficiently kill influenza virus-infected lung alveolar epithelial cells. Cell. Mol. Immunol. *10*, 159–164.

Lim, W.H., Kireta, S., Russ, G.R., and Coates, P.T. (2007). Human plasmacytoid dendritic cells regulate immune responses to Epstein-Barr virus (EBV) infection and delay EBV-related mortality in humanized NOD-SCID mice. Blood *109*, 1043–1050.

Long, H.M., Taylor, G.S., and Rickinson, A.B. (2011). Immune defence against EBV and EBV-associated disease. Curr. Opin. Immunol. *23*, 258–264.

Louis, C.U., Straathof, K., Bollard, C.M., Gerken, C., Huls, M.H., Gresik, M.V., Wu, M.F., Weiss, H.L., Gee, A.P., Brenner, M.K., et al. (2009). Enhancing the in vivo expansion of adoptively transferred EBV-specific CTL with lymphodepleting CD45 monoclonal antibodies in NPC patients. Blood *113*, 2442–2450.

Ma, S.D., Hegde, S., Young, K.H., Sullivan, R., Rajesh, D., Zhou, Y., Jankowska-Gan, E., Burlingham, W.J., Sun, X., Gulley, M.L., et al. (2011). A new model of Epstein-Barr virus infection reveals an important role for early lytic viral protein expression in the development of lymphomas. J. Virol. *85*, 165–177.

Orsini, D.L., van Gils, M., Kooy, Y.M., Struyk, L., Klein, G., van den Elsen, P., and Koning, F. (1994). Functional and molecular characterization of B cell-responsive V delta 1+ gamma delta T cells. Eur. J. Immunol. *24*, 3199–3204.

Puan, K.J., Jin, C., Wang, H., Sarikonda, G., Raker, A.M., Lee, H.K., Samuelson, M.I., Märker-Hermann, E., Pasa-Tolic, L., Nieves, E., et al. (2007). Preferential recognition of a microbial metabolite by human Vgamma2Vdelta2 T cells. Int. Immunol. *19*, 657–673.

Qin, G., Mao, H., Zheng, J., Sia, S.F., Liu, Y., Chan, P.L., Lam, K.T., Peiris, J.S., Lau, Y.L., and Tu, W. (2009). Phosphoantigen-expanded human gammadelta T cells display potent cytotoxicity against monocyte-derived macrophages infected with human and avian influenza viruses. J. Infect. Dis. *200*, 858–865.

Qin, G., Liu, Y., Zheng, J., Ng, I.H., Xiang, Z., Lam, K.T., Mao, H., Li, H., Peiris, J.S., Lau, Y.L., and Tu, W. (2011). Type 1 responses of human Vγ9Vδ2 T cells to influenza A viruses. J. Virol. *85*, 10109–10116.

Qin, G., Liu, Y., Zheng, J., Xiang, Z., Ng, I.H., Malik Peiris, J.S., Lau, Y.L., and Tu, W. (2012). Phenotypic and functional characterization of human γδ T-cell subsets in response to influenza A viruses. J. Infect. Dis. *205*, 1646–1653.

Rooney, C.M., Smith, C.A., Ng, C.Y., Loftin, S., Li, C., Krance, R.A., Brenner, M.K., and Heslop, H.E. (1995). Use of gene-modified virus-specific T lymphocytes to control Epstein-Barr-virus-related lymphoproliferation. Lancet *345*, 9–13.

Shapiro, R.S., McClain, K., Frizzera, G., Gajl-Peczalska, K.J., Kersey, J.H., Blazar, B.R., Arthur, D.C., Patton, D.F., Greenberg, J.S., Burke, B., et al. (1988). Epstein-Barr virus associated B cell lymphoproliferative disorders following bone marrow transplantation. Blood *71*, 1234–1243.

Sicard, H., Ingoure, S., Luciani, B., Serraz, C., Fournié, J.J., Bonneville, M., Tiollier, J., and Romagné, F. (2005). In vivo immunomanipulation of V gamma 9V delta 2 T cells with a synthetic phosphoantigen in a preclinical nonhuman primate model. J. Immunol. *175*, 5471–5480.

Speck, P., and Longnecker, R. (1999). Epstein-Barr virus (EBV) infection visualized by EGFP expression demonstrates dependence on known mediators of EBV entry. Arch. Virol. *144*, 1123–1137.

Strowig, T., Brilot, F., Arrey, F., Bougras, G., Thomas, D., Muller, W.A., and Münz, C. (2008). Tonsilar NK cells restrict B cell transformation by the Epstein-Barr virus via IFN-gamma. PLoS Pathog. *4*, e27.

Tu, W., Zheng, J., Liu, Y., Sia, S.F., Liu, M., Qin, G., Ng, I.H., Xiang, Z., Lam, K.T., Peiris, J.S., and Lau, Y.L. (2011). The aminobisphosphonate pamidronate controls influenza pathogenesis by expanding a gammadelta T cell population in humanized mice. J. Exp. Med. *208*, 1511–1522.

Tzartos, J.S., Khan, G., Vossenkamper, A., Cruz-Sadaba, M., Lonardi, S., Sefia, E., Meager, A., Elia, A., Middeldorp, J.M., Clemens, M., et al. (2012). Association of innate immune activation with latent Epstein-Barr virus in active MS lesions. Neurology *78*, 15–23.

Wagner-Johnston, N.D., and Ambinder, R.F. (2007). Epstein-Barr virus-related lymphoproliferative disorders. Curr Hematol Malig Rep *2*, 249–254.

Zheng, J., Liu, Y., Lau, Y.L., and Tu, W. (2013a). γδ-T cells: an unpolished sword in human anti-infection immunity. Cell. Mol. Immunol. *10*, 50–57.

Zheng, J., Liu, Y., Liu, M., Xiang, Z., Lam, K.T., Lewis, D.B., Lau, Y.L., and Tu, W. (2013b). Human CD8+ regulatory T cells inhibit GVHD and preserve general immunity in humanized mice. Sci Transl Med *5*, 168–169.